JOURNAL OF CATALYSIS 119, 161–178 (1989)

Methane Oxidative Coupling

II. A Study of Lithium–Titania-Catalyzed Reactions of Methane

GERALD S. LANE,[1] EDUARDO MIRO,[2] AND EDUARDO E. WOLF[3]

Department of Chemical Engineering, University of Notre Dame, Notre Dame, Indiana 46556

Received October 21, 1988; revised May 5, 1989

Methane conversion to higher hydrocarbons via oxidative coupling was studied on a series of lithium-doped titania catalysts by cofeeding methane and oxygen. The degree of lithium promotion was studied by varying the lithium loading from 0 to 31.7 wt% lithium on the rutile crystal structure of titania. Catalytic results indicate that lithium-doped titania catalysts are effective for oxidative coupling of methane with hydrocarbon product selectivities ranging from 20 to 85%. Increasing the lithium loading reduces the combustion activity of the catalyst, improves hydrocarbon selectivity, and increases space-time yields. Product yield reached a maximum for the 16.2-wt% loading; this catalyst had methane conversions of ca. 15% with hydrocarbon selectivities of ca. 75%. The 16.2-wt% lithium–titania catalyst was studied under various operating conditions and compared favorably with other catalytic results that have been reported. The observed activation energy of the 16.2% lithium–titania catalyst was dependent on the reactant partial pressure and ranged from 25.6 to 37.6 kcal/mole. X-ray diffraction, X-ray photoelectron spectroscopy, infrared analysis, and differential thermal analysis results of the catalysts indicate that increasing the degree of lithium promotion lowers the surface area and the surface concentration of oxygen, and creates different phases at elevated temperatures. Routes for surface-catalyzed reactions coupled with gas-phase reactions were studied by transient pulse and step-change experiments. The transient experiments suggest that adsorbed oxygen is responsible for the C_2 hydrocarbon activity of the lithium–titania catalyst and that lattice oxygen activates methane nonselectively.

INTRODUCTION

Although the oxidative coupling of methane gives predominantly ethane and ethylene, not the desired final products of methane utilization, the process has become an active research area, and some success has been achieved. In 1982 a survey of oxidative coupling catalysts was first reported by Keller and Bhasin (*1*); numerous reports have since been published on the oxidative coupling of methane. Some of the initial studies have been recently reviewed by Lane (*2*), Bhasin (*3*), Mimoun (*4*), Roos *et al.* (*5*), Scurrell (*6*), and Lee and Oyama (*7*). Methane oxidative coupling reactions are usually operated under atmospheric pressure using diluted feeds and in the temperature range 600 to 900°C.

Two approaches have been used in these oxidative coupling studies to give higher hydrocarbons: cyclic feeding operation and cofeeding operation. In cyclic feeding, methane and oxygen are fed alternatively to minimize the conversion of methane in the gas phase and to minimize sequential combustion of hydrocarbon products. Oxygen of the metal–oxide lattice participates in a redox cycle similar to the Mars–van Krevelen mechanism (*8*). Several authors have reported results using this technique and have shown that fairly good activities and product selectivities can be achieved (*1, 9–13*).

The most active area of methane utilization research involves the continuous cofeeding of methane and oxygen. By cofeeding methane and oxygen, gas-phase

[1] Amoco Oil Co., Amoco Research Center, P.O. Box 400, Naperville, IL 60566.

[2] On leave from Conicet, Santa Fe, Argentina

[3] To whom correspondence should be addressed.

0021-9517/89 $3.00

reactions can become significant. Lane and Wolf (*14*) were among the first to extensively study the importance and role of gas-phase oxidative coupling of methane, and recently other reports have also demonstrated the importance of gas-phase reactions (*15–17*). Gas-phase reactions become significant at reactant partial pressures higher than 0.4, long residence times, and high temperatures (*14*). Several research groups using a variety of catalysts and less severe operating conditions have reported fairly high hydrocarbon yields in their catalytic studies.

Most of the research on methane utilization has been directed at the identification of suitable catalysts which give high yields of higher hydrocarbons. Numerous combinations of elements have been tested for their oxidative coupling activity. The compounds are typical oxides, but various combinations of oxides, carbonates, nitrates, sulfates, and hydroxides have been tested. The effects of alkali and halide compounds as promoters have also been tested by several groups.

In this study, the oxidative coupling of methane was studied using a series of lithium-doped titania catalysts by cofeeding methane and oxygen. The objective of this study was to determine the effect of lithium on lithium–titania catalysts in relation to the homogeneous study discussed elsewhere (*14*). The rutile crystal structure of titania was chosen to be the catalyst material since it was thought to give up oxygen during CO oxidation (*18*). Lithium has been shown to be an effective promoter for the oxidative coupling of methane (*19, 20*) and was chosen to promote the titania. The degree of promotion was studied by varying the lithium loading from 0.0 to 31.7% on the rutile crystal structure of titania. Limited results on lithium–titania catalysts have been reported by Kolts and Kimble (*21*) showing these catalysts to have some catalytic activity at high molar feed ratios of methane-to-oxygen, ~15. Experiments were performed under operating conditions which minimize gas-phase conversion and under conditions in which the gas-phase reactions compete with surface-catalyzed reactions. Transient experiments were also performed to identify the importance of lattice oxygen, adsorbed oxygen, and gas-phase oxygen. Catalyst characterization techniques were combined with kinetic measurements to correlate the role of lithium promotion with activity in the oxidative-coupling reaction pathway.

EXPERIMENTAL

Kinetic measurements were performed using single-pass flow reactors made of fused silica with inside diameters of 0.95 cm and with heated lengths of 15 cm. The details of this apparatus have been given elsewhere (*2*); therefore, only a brief description is given here. The reactors were heated resistively with a furnace designed and built to minimize the heated length. The temperature of the reactor was monitored by a K-type thermocouple placed in a quartz thermocouple well and controlled by an Omega 2012 programmable temperature controller. The flow rate of each component in the feed was controlled and regulated by electronic mass flow controllers (Brooks Instrument Co.). The gases, used as delivered without purification, were ultrahigh purity grades obtained from Linde Specialty Gases and were of the following purities: CH_4 (99.97%), O_2 (99.99%), and He (99.999%).

Product analyses were performed by on-line gas chromatography (GC) using a thermal conductivity detector on a Carle GC (model AGC 111) equipped with thermistors. The major products were C_2H_6, C_2H_4, C_3H_8, C_3H_6, CO, CO_2, H_2, and H_2O. Water was removed from the reaction products by a trap placed at the reactor exit to eliminate the presence of a broad water peak from the GC analysis. Two columns operated in parallel to achieve sufficient separation of the products and reactants: a Carbosphere-packed column ($\frac{1}{8}$ in. × 6 ft) was used for the separation of H_2, O_2, CH_4, CO, and CO_2,

and a HayeSep Q polymer-packed column ($\frac{1}{8}$ in. × 6 ft), was used for the separation of CO_2, C_2H_6, C_2H_4, C_3H_6, and C_3H_8. Feed and effluent gas mixtures were sampled by two in-line six-way sampling valves (Carle Chromatograph). Gas compositions were calculated using external standards as shown elsewhere (*2*). The closures on the carbon mass balances were within 2% and in most cases were within 1%; hydrogen and oxygen mass balances typically closed within 2% based on overall mass balances. Effluent flow rates were measured with a bubble meter at the exit of the GC sample loops to correct for the change in the number of moles due to reaction and condensation of products in the cold trap.

Typical operating conditions used to compare the activity of the catalysts were as follows: atmospheric pressure, a 250-mg sample loading of catalyst, a partial pressure of methane and oxygen divided by the total pressure of 0.4, a feed flow rate at ambient conditions of 100 cc/min, a methane-to-oxygen feed mole ratio of 4, and temperatures from 600 to 800°C. The methane and oxygen conversions and product selectivities were typically compared after 2 h time-on-stream.

The transient experiments were performed by sending pulses or step changes of various gas mixtures over 100 mg or 0.5g of the 16.2% lithium–titania catalyst at 750°C. The reaction products at various times after the feed change were collected in a multiport sample valve. The products were then analyzed by gas chromatography. Pulses were typically on the order of 0.5 ml.

The rutile crystal structure of titania was prepared by a 12-h 800°C hydrogen reduction of Degussa P-25 TiO_2 which was followed by a 2-h calcination in flowing oxygen at 600°C. This treatment is given in detail in elsewhere (*18*) where it was shown that the resulting titania predominantly has the rutile crystal structure (greater than 96% rutile). The lithium-doped titania catalysts were prepared by combining lithium oxide (Alfa Products) and rutile titania in deionized water and evaporating the water at 40°C while stirring until dry (~24 h). Each catalyst was calcined at 600°C in flowing O_2 for 2 h and then stored until use. Before each activity measurement, the catalyst was again calcined for 2 h by ramping the temperature from room temperature to 600°C over the first $\frac{1}{2}$ h and then holding at 600°C for $1\frac{1}{2}$ h. The reactor was then cooled, and the reaction gases were mixed and fed to the reactor. A sample was taken at room temperature, and then the reactor temperature ramped to the reaction temperature using the programmable temperature controller. A different fused-silica reactor was used for each catalyst sample due to the apparent formation of lithium silicate on the reactor walls. A series of catalysts was prepared by using the method mentioned above, and the degree of promotion is given in weight percentage defined as the ratio of lithium to the sum of Li_2O and TiO_2. The results of several catalysts with lithium weight loadings of 0.0, 1.0, 3.8, 6.7, 11.0, 16.2, and 31.7% are presented.

Several techniques were combined to characterize the catalyst samples. The BET surface area of each catalyst was measured after calcination but prior to reaction by a Quantachrome QS-8 unit, using the flow adsorption method described elsewhere (*2*), with N_2 as the adsorbing gas and helium as the carrier gas. The diffraction pattern of each catalyst was measured using a Diano XPG-2 X-ray diffractometer with Cu$K\alpha$ radiation (λ = 1.542 Å), a 3° beam slit, and a 0.2° detector slit. The X-ray diffraction (XRD) samples were pressed wafers of the catalyst materials which were mounted on glass slides. The x-ray photoelectron spectroscopy (XPS) analyses of calcined catalyst were performed using a 5950B ESCA spectrometer in collaboration with Dr. T. H. Fleisch at the Amoco Research Center. Differential thermal analysis, described in detail by Wendlandt (*27*) and Smothers and Chiang (*28*), provides a qualitative and semiquantitative measure of the heat ef-

fects associated with physical and chemical changes. The 16.2% lithium–titania catalyst was analyzed by differential thermal analysis (DTA) using a Fisher differential thermalyzer 260P, and outputs were recorded on a Honeywell Electronik 194 recorder at 0.2 mV full-scale. Two ceramic insulated K-type thermocouples were wired to give differential temperature measurements. The sample and reference material (γ-alumina) were dried, and quartz crucibles were filled with 200 mg of material. The samples were heated from room temperature to 850°C and then allowed to cool.

RESULTS

Activity–Selectivity Results

A comparison of kinetic measurements with and without catalyst by Lane and Wolf reported elsewhere (*22*) shows that gas-phase results compare favorable with catalytic results over the lithium–titania catalyst under high reactant partial pressures. Under other conditions, catalytic reactions generate the majority of the products. The following studies have been conducted under conditions which minimize the gas-phase reactions.

(*a*) *Effect of Catalyst Loading on Activity*

The degree of lithium promotion was varied from 0.0 to 31.7% on the rutile crystal structure of titania to see if product selectivity could be improved. In order to observe the catalytic activity, the operating conditions were chosen to minimize gas-phase conversion. The conditions were chosen based on the results presented elsewhere (*14*) which indicate that the gas-phase conversion would be minimal if the following conditions were used: a feed flow rate of 100 cc/min at ambient conditions, a CH_4/O_2 feed mole ratio equal to 4, and a reactant partial pressure of 0.4. To obtain significant conversion, the activity measurements were carried out at 800°C using 250 mg of catalyst. Each catalyst was pretreated in flowing O_2 for 2 h at 600°C and cooled in helium before activity measurements were begun. Figures 1a and 1b compare the hydrocarbon and carbon oxide yields for each catalyst measured after 2 h time-on-stream under the conditions specified above. Yield has been defined as the amount of carbon converted to a given product divided by the amount of carbon fed and has been expressed as a percentage. The first seven bars depicted in Figs. 1a and 1b show the effects of increasing the lithium loading, whereas the last bar shows gas-phase results for comparison. When the lithium loading was increased from 0 to 11%, methane conversion fell from 20 to nearly 5%, whereas, the hydrocarbon selectivity increased as conversion de-

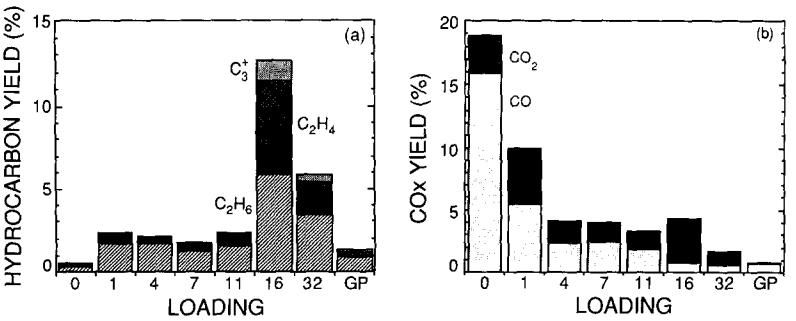

FIG. 1. Comparison of hydrocarbon and carbon oxide yields for a series of lithium-promoted titania catalysts. Results are also compared for gas-phase reactions. The results represent samples taken at 800°C after 2 h time-on-stream with a CH_4/O_2 feed mole ratio of 4, a feed flow rate of 100 cc/min, a 250-mg catalyst sample, and a reactant partial pressure of 0.4.

creased. Coupled with this decrease in methane conversion was a lowered level of oxygen conversion as it fell from nearly 100 to ca. 25%. Both methane and oxygen conversion decreased by a factor of 4 with increased lithium loading, and the ratio of conversions remained ca. 4. The resulting hydrocarbon yield (i.e., conversion times selectivity) remained beteen 2 and 3% except for the 16.2% lithium–titania catalyst which was around 12.5%.

The 16.2% lithium–titania catalyst exhibits higher methane and oxygen conversions leading to higher hydrocarbon yields than would be predicted by the trend of other loadings. Two additional batches of this catalyst were prepared, and all three batches showed this anomaly in methane and oxygen conversions. At these higher conversions, the ratio of oxygen conversion to methane conversion has decreased from 4, observed for the other loadings, to about $2\frac{1}{2}$. With these higher conversions, the 16.2% lithium catalyst has reasonably high product selectivities for hydrocarbons, 75%, indicating that this catalyst has active sites for the generation of the desired hydrocarbon products. A 31.7% lithium–titania catalyst was prepared after observing the high activity of the 16.2% lithium loading. The results of this catalyst are also summarized in Figs. 1a and 1b and show that it also has higher activity than the trend predicted by the 0.0 to 11% catalyst loadings; however, the activity of the 31.7% lithium–titania catalyst was less than the 16.2% loading, possibly due to less catalyst surface area. Figures 1a and 1b also show that the operating conditions are such that gas-phase reactions have not been completely eliminated, as shown by the last bar displayed in this figure.

Results, for the 1-11% lithium–titania catalysts show that the increased hydrocarbon product selectivity compensates for the decreased methane conversion, and the hydrocarbon yields remain constant at ca. 2%. The 16.2 and 31.7% lithium–titania catalysts have much higher hydrocarbon yields than the other catalysts. Owing to this higher yield, the 16.2% catalyst was studied in more detail.

(*b*) *Additional Results on 16.2% Lithium–Titania Catalyst*

Three batches of the 16.2% lithium–titania catalyst all showed similar activity. To see if there was any effect from using another precursor other than Li_2O, a 16.2% lithium–titania catalyst was prepared using Li_2CO_3 as the precursor. At 2 h time-on-stream, this catalyst showed similar conversions and product selectivities observed for the catalyst prepared with Li_2O. The catalyst was also pretreated under oxidizing, reducing, and CO_2 pretreatments prior to reaction. Pretreatment only affected the initial activity, and after 2 h time-on-stream the pretreatment had very little effect. Larkins and Nordin (*23*) and Otsuka *et al.* (*24*) also conclude that little difference is observed in using LiOH and Li_2CO_3 and Li_2O and Li_2CO_3, respectively. Since little effect on activity and selectivity was observed using different lithium precursors and various pretreatments, subsequent studies were performed using the 16.2% lithium–titania catalyst prepared with the Li_2O precursor after a 2-h 600°C calcination pretreatment.

Effect of reactant partial pressure. The effect of the degree of reactant dilution was studied by varying the reactant partial pressures over the 16.2% lithium–titania catalysts. Figure 2 reflects the results of this study and shows that reactant partial pressure does not greatly affect conversion or product selectivity as it did in the gas-phase reactions as shown elsewhere (*14*). Only at high reactant partial pressure does the influence of gas-phase reactions become slightly apparent with an increase in CO selectivity. The effect of reactant partial pressure on the 16.2% lithium–titania catalyst is similar to that of other loadings.

Effect of contact time. Figures 3a and 3b display the influence of contact time on conversion and product selectivity results

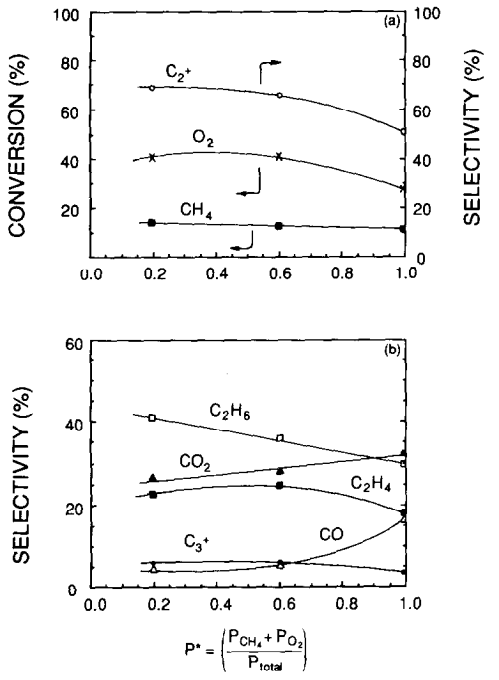

FIG. 2. The effect of the reactant partial pressure on CH_4 and O_2 conversions and on product selectivities at 750°C using 250 mg of 16.2% lithium–titania catalyst with a feed mole ratio of CH_4/O_2 of 4 and with a total feed flow rate of 100 cc/min; (a) shows methane and oxygen conversions and total hydrocarbon product selectivity, and (b) shows product distribution.

at 700°C using the 16.2% lithium–titania catalyst. In this study, contact time was varied by changing the catalyst loading and keeping the volumetric feed flow rate constant. Extrapolation of the product selectivities to zero contact time in Fig. 3b shows that ethane and CO_2 would be the major products observed. This indicates that ethane and CO_2 are initial products, and ethylene and possibly CO are produced as secondary products. This is quite different from the residence time study of the gas-phase reactions (*14*), where it was found that only ethane would be formed at zero residence time.

Temperature effects. Figures 4a and 4b display the variation in methane and oxygen conversions and product selectivities with changing temperature. Over the temperature range with this set of operating conditions, the conversions were nondifferential. The trends shown in Fig. 4b are similar to other catalytic studies showing improved higher hydrocarbon selectivity with increasing temperature. A substantial gain in ethane production was observed between the 650 and 700°C results. It was observed that the postrun catalyst samples from the experiments performed at 700°C or higher had experienced a change in their physical state. This change of state was then investigated by XRD and differential thermal analysis (DTA) to see if there was a phase change, and these results will be described with the other characterization results.

Differential rates, where conversions were less than 10%, were used to fit the influence of temperature to an Arrhenius-type dependence for the 16.2% lithium–titania catalyst. This was done for both low, $P^* = 0.2$, and high reactant partial pressure

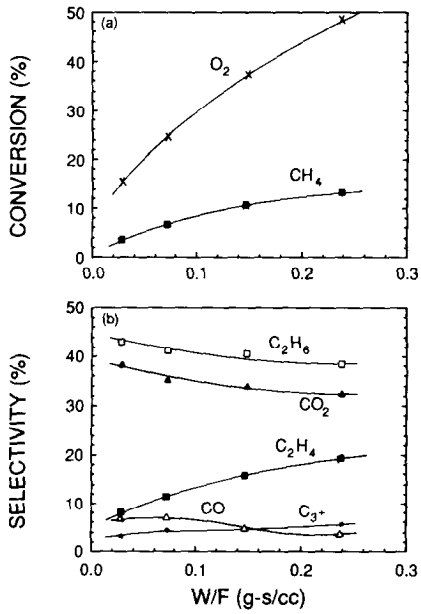

FIG. 3. The effect of contact time on CH_4 and O_2 conversions and on product selectivities at 700°C using the 16.2% lithium–titania catalyst with a feed mole ratio of CH_4/O_2 of 4, a constant feed flow rate of 100 cc/min, and a partial pressure of reactants of 0.4; (a) shows methane and oxygen conversions, and (b) shows product selectivity.

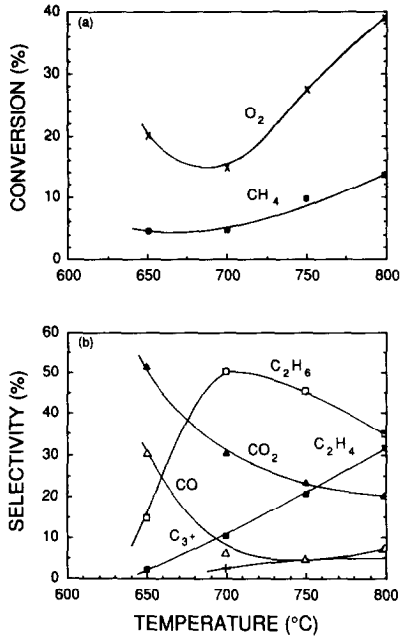

FIG. 4. Temperature effects on CH_4 and O_2 conversions and product selectivities using 250 mg of 16.2% lithium–titania catalyst with a feed flow rate of 100 cc/min, a feed mole ratio CH_4/O_2 of 4, and a partial pressure of reactants of 0.4; (a) shows methane and oxygen conversions, and (b) shows product selectivity.

ratios, $P^* = 0.8$, to see the influence of gas-phase reactions on the observed activation energy. At a reactant partial pressure of 0.2, the apparent activation energy for ethane formation was 25.6 kcal/mole, whereas at a reactant partial pressure of 0.8 where gas-phase reactions become important, the apparent activation energy was 37.6 kcal/mole. In the absence of a catalyst, the observed activation energy for ethane formation was 51.8 kcal/mole (*14*). Thus, the activation energy determined at high reactant partial pressures includes the influence of temperature on both the catalytic and gas-phase reactions.

Time-on-stream. Since the 16.2% titania–lithium catalyst appeared to have some of the features necessary for oxidative coupling, the catalyst was studied for 48 h. Changes in product hydrocarbon yields are shown in Fig. 5, indicating that the catalyst loses activity with time-on-stream, similar to results reported by Korf *et al.* (*25*) for a Li/MgO catalyst. A possible reason for some of the loss in catalytic activity would be a loss of lithium. A loss of lithium could be explained by three possibilities: (i) lithium has a relatively high solubility in water (a reaction product), (ii) the vapor pressure of lithium and lithium hydroxide is not negligible at 800°C, and (iii) some of the lithium forms lithium silicate with the fused-silica walls of the reactor. A solution to the deactivation problem was not investigated, but the time-on-stream study provides several insights into the reaction pathway.

As the catalyst deactivated, the gas-phase reactions began to dominate the reaction process, and after 48 h time-on-stream, the methane conversion and product selectivity reflected those observed for the gas-phase reactions. The only exception was that the catalyst produced more CO_2 and less CO than in the gas phase. Table 1 compares the space-time yields at short and long reaction times with those observed for gas-phase reactions. The catalyst converted more methane with better hydrocarbon selectivity than would be obtained by gas-phase-controlled reactions. At short

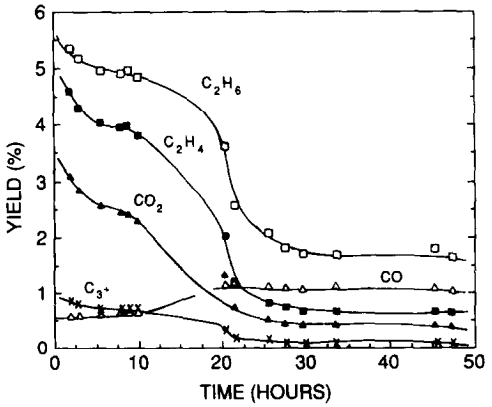

FIG. 5. Effects of time-on-stream for the 16.2% lithium–titania catalyst at 800°C for a CH_4/O_2 feed mole ratio of 4, a 250-mg catalyst sample, a feed flow rate of 100 cc/min, and a reactant partial pressure of 0.4; hydrocarbon yields and carbon oxide yields are shown.

TABLE 1

Space-Time Yield at 800°C[a]

Product	2 h[b]		47 h[b]		Gas phase	
	STY[c] $\left(\frac{\mu\text{mole}}{\text{min}}\right)$	Selectivity (%)	STY[c] $\left(\frac{\mu\text{mole}}{\text{min}}\right)$	Selectivity (%)	STY[c] $\left(\frac{\mu\text{mole}}{\text{min}}\right)$	Selectivity (%)
C_2H_6	68.8	37	19.6	45	11.3	42
C_2H_4	59.2	32	7.2	16	4.1	15
C_3^+	10.6	6	0.6	1	1.7	6
CO_2	39.8	21	4.2	10	0.3	1
CO	7.6	4	12.3	28	9.6	36
Total	186.0	100	43.9	100	27.0	100

[a] $CH_4/O_2 = 4$, $P^* = 0.4$, $Q = 100$ cc/min (room temperature).
[b] 250-mg initial catalyst loading measured at different times-on-stream.
[c] Space-time yield defined as micromole CH_4 to a given product per minute.

time-on-stream, the space-time yield for methane conversion was approximately six times greater than that in the gas phase. Over the 48-h period shown in Fig. 5, the catalyst lost about 75% of its activity and the hydrocarbon product selectivity decreased from 75 to 62%. A major portion of the loss in activity can be attributed to an eight to tenfold decrease in the space-time yields for CO_2 and C_2H_4 production. This indicates that the catalyst is at least partially responsible for the generation of these products.

Transient Experimental Results

In order to investigate the reactivity of lattice and adsorbed oxygen, several pulsing and step-change experiments were conducted. In one of these experiments, the 16.2% lithium–titania catalyst was heated to 750°C. After the temperature had stabilized, methane was flowed over the catalyst; 30 s after starting the flow of methane, a pulse of 2% oxygen was fed along with methane. Figure 6 displays the results of this experiment showing the products formed in volume percent. In the first part of the experiment, with methane-only feed, the lattice oxygen produces mainly CO and only trace amounts of ethane and ethylene. When the 2% oxygen is allowed into the system, the production of CO decreases, and the production of ethane and ethylene increases. The decrease in CO production is probably due in part to the formation of surface carbonates following the production of CO_2 on the surface. In a second experiment, a 0.5-ml pulse of oxygen, fol-

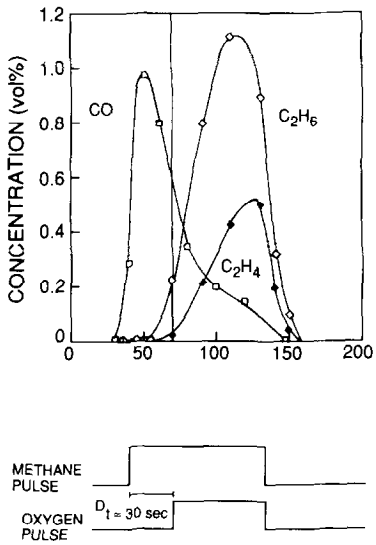

FIG. 6. Reactivity of lattice and adsorbed oxygen after out-of-phase step changes in CH_4 and O_2 over 500 mg of the 16.2% lithium–titania catalyst at 750°C; $W/F = 1.6 \times 10^{-3}$ g min/cc.

lowed by a 0.5-ml pulse of methane, was fed over the catalyst. The pulsed methane reacted with the adsorbed oxygen, which was retained from the previous oxygen pulse, to produce ethane and ethylene as shown in Fig. 7. Figure 7 also shows that the ratio of ethane to ethylene is high (ca. 10) and remains approximately constant. In this experiment CO and CO_2 could not be detected because only an FID detector was used. Some CO must have been present but not CO_2 since it is adsorbed as carbonate.

A third set of experiments was performed by sending pulses of methane and varying amounts of oxygen, 0 to 5.1%, over the catalyst at 750°C. In these pulse experiments the reactants and products flowed directly into the gas chromatograph; consequently the concentrations measured represent the amount accumulated during the duration of the pulse. Figure 8 summarizes the results of this set of experiments. In these experiments, like those shown in Fig. 6, no CO_2 is detected in the effluent. The

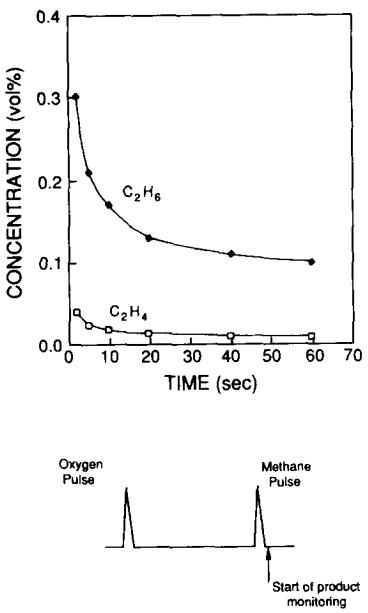

FIG. 7. Volume percent ethane and ethylene after a 0.5-ml methane pulse following a 0.5-ml pulse of oxygen over 500 mg of the 16.2% lithium–titania catalyst at 750°C.

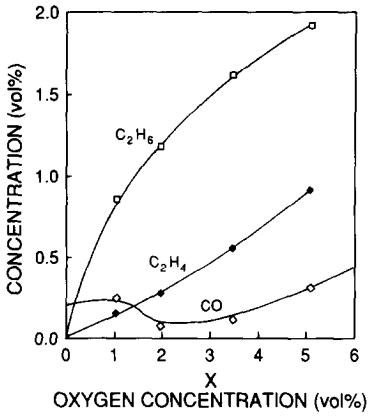

FIG. 8. Methane pulsing at various oxygen concentrations over 100 mg of the 16.2% lithium–titania catalyst at 750°C; $CH_4:O_2:He = (100-X):X:0$, $W/F = 1.7 \times 10^{-4}$ g min/cc.

carbon balance does not close, and temperature-programmed desorption analysis indicates that small amounts of CO_2 desorb from the surface of the catalyst following these types of experiments. Figure 8 shows that the product ethane and ethylene increases with the amount of oxygen, whereas the CO which was shown in Fig. 6 to result from a reaction with lattice oxygen is rather insensitive to the amount of oxygen being fed.

Two sets of experiments similar to those shown in Fig. 8 were conducted with ethane and ethylene pulsed instead of methane. Figures 9a and 9b show the results for the ethane and ethylene experiments, respectively. In Fig. 9a, it is apparent that ethane is readily dehydrogenated to ethylene with either lattice, adsorbed, or gas-phase oxygen, with the product distribution being almost independent of the oxygen concentration. Figure 9b shows that ethylene is converted to a lesser extent (ca. 20%) than is ethane in the experiment shown in Fig. 9a (ca. 50%). Both carbon and oxygen balances in the ethylene experiments indicate that CO_2 must be the major product from the reaction of ethylene, but the CO_2 remains on the catalyst in the form of a carbonate and is not detected in the effluent.

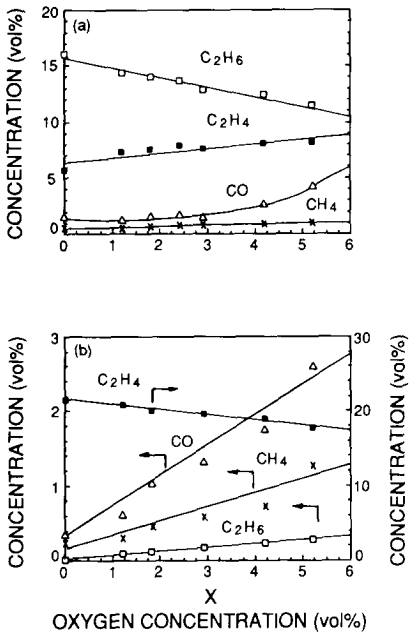

FIG. 9. (a) Ethane pulsing using 0.5-ml pulses at various oxygen concentrations over 100 mg of the 16.2% lithium–titania catalyst at 750°C; $C_2H_6:O_2:He = 22.5:X:(77.5-X)$, $W/F = 1.7 \times 10^{-4}$ g min/cc. (b) Ethylene pulsing using 0.5-ml pulses at various oxygen concentrations over 100 mg of the 16.2% lithium–titania catalyst at 750°C; $C_2H_4:O_2:He = 22.5:X:(77.5-X)$, $W/F = 1.7 \times 10^{-4}$ g min/cc.

CATALYST CHARACTERIZATION RESULTS

To gain some insight into the active species, the catalysts were characterized by XRD, XPS, DTA, and use of diffuse reflectance infrared spectroscopy. The results of the BET area measurements show that the total surface area decreases with increasing lithium loading. This indicates that in a comparison of the effects of lithium loading shown in Fig. 1a and 1b, the change in activities and product selectivities are also due to decreasing surface area.

X-Ray Diffraction

Figure 10 shows the diffraction patterns of six of the lithium–titania catalysts and compares these with Li_2TiO_3. The samples were also analyzed on a computerized X-ray diffractometer by Dr. Kaduk at the Amoco Research Center. The computer identified the major and minor crystal structure present in each catalyst (summarized in Table 2). Table 2 shows that the Li_2O precursor was not detected in the catalyst and that the crystal structure of lithium titanate becomes the dominate crystal structure present at high lithium loadings. The 16.2% lithium–titania catalyst was the only catalyst in which the computer identified the presence of $LiTiO_2$. It should be pointed out that the XRD analysis was performed at room temperature and with exposure to air.

X-Ray Photoelectron Spectroscopy

Table 3 summarizes the electron binding energies of the elements detected on the catalysts at different lithium loadings. The C 1*s* and O 1*s* spectra gave evidence that multiple carbon and oxygen species were present on the catalyst surface. Table 3 also

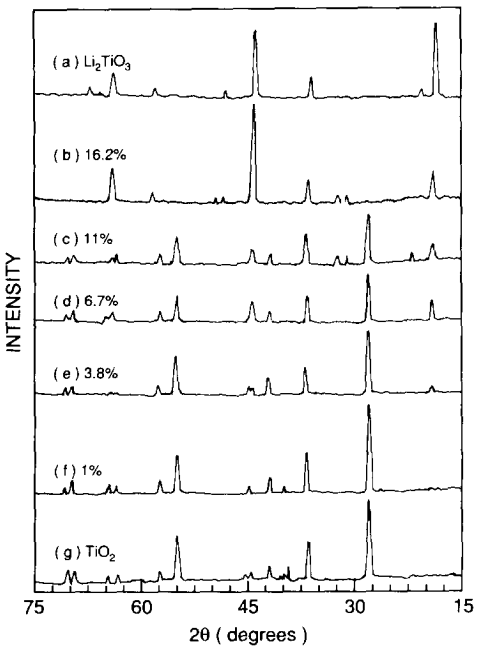

FIG. 10. X-ray diffraction patterns of lithium–titania catalysts after 600°C calcination pretreatment; (a) Li_2TiO_3, (b) 16.2% Li/TiO_2, (c) 11.0% Li/TiO_2, (d) 6.7% Li/TiO_2, (e) 3.8% Li/TiO_2, (f) 1% Li/TiO_2, and (g) rutile titania.

TABLE 2

Crystal Structures for the Lithium–Titania Catalysts as Detected by X-ray Diffraction

Catalyst	XRD phases present				
	TiO_2	LiO_2	Li_2TiO_3	Li_2CO_3	$LiTiO_2$
Rutile TiO_2	Major	*nd*	*nd*	*nd*	*nd*
1% Li_2O/TiO_2	Major	*nd*	Minor	*nd*	*nd*
4% Li_2O/TiO_2	Major	*nd*	Minor	*nd*	*nd*
7% Li_2O/TiO_2	Major	*nd*	Major	*nd*	*nd*
11% Li_2O/TiO_2	Major	*nd*	Major	Minor	*nd*
16% Li_2O/TiO_2	Minor	*nd*	Major	Minor	Major
Li_2TiO_3	*nd*	*nd*	Major	*nd*	*nd*

Note. *nd* indicates not detected.

includes the relative percentages of the integrated intensities of each of the carbon and oxygen species. Figure 11 shows the spectra of the O 1*s* species, indicating that the higher binding-energy species grows relative to the lower binding-energy O 1*s* species as the loading of lithium is increased. The higher binding-energy oxygen species relates to the presence of carbonate-type oxygen, and higher binding-energy oxygen species have been reported by France *et al.* (*26*) to give higher C_2^+ selectivities. The various C 1*s* species have been associated with the following: (i) a

TABLE 3

Electron Binding-Energy Results for the Lithium–Titania Catalysts[a]

Catalyst	Electron binding energy (eV)					
	Ti $2p_{\frac{3}{2}}$	Li 1*s*	O 1*s*	%	C 1*s*	%
Rutile TiO_2	458.0	—	529.4	72	284.8	79
			530.5	28	286.6	9
					288.6	13
1% Li_2O/TiO_2	458.0	54.9	529.2	71	284.5	68
	530.8	29	286.4	13		
			288.3	19		
4% Li_2O/TiO_2	458.0	54.6	529.4	66	284.5	62
	530.9	34	285.9	15		
			288.9	23		
7% Li_2O/TiO_2	458.0	54.5	529.3	53	284.3	46
	530.9	47	285.9	18		
			287.9	11		
			287.3	20		
11% Li_2O/TiO_2	458.0	54.6	529.2	56	284.7	44
	531.1	44	286.5	27		
			288.1	11		
			289.6	18		
16% Li_2O/TiO_2	458.0	54.6	529.3	23	284.7	41
			531.3	77	286.6	18
					289.4	41

[a]Binding energies referenced against Ti $2p_{\frac{3}{2}}$ = 458.0 eV.

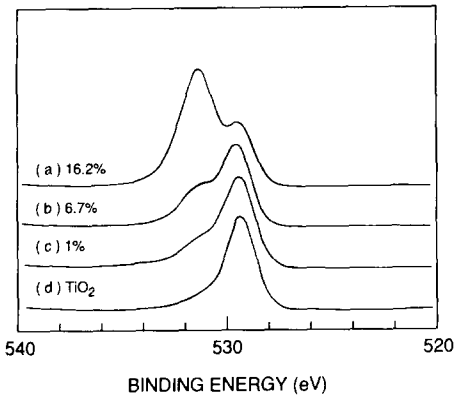

FIG. 11. Changes in O 1*s* binding-energy spectra of the lithium–titania catalyst with different lithium loadings. Binding energies referenced against the Ti $2p_{\frac{3}{2}}$ = 458.0 eV; (a) 16.2% lithium–titania catalyst, (b) 6.7% lithium–titania catalyst, (c) 1% lithium–titania catalyst, and (d) rutile titania.

binding energy of 284.6 eV corresponds to graphite or hydrocarbons; (ii) a binding energy of 286 eV corresponds to C–O species; (iii) a binding of 287–288 eV could indicate C = O; and (iv) carbonates are usually observed ca. 289 eV.

Table 4 summarizes the surface composition as measured by XPS. The ratio of O-to-(Li + Ti) decreased with increasing lithium loading, suggesting that the lithium loading controls the amount of surface oxygen. It should be pointed out that the surface concentration of oxygen measured by XPS is much higher than would be estimated by the bulk composition which is shown in parentheses in Table 4. The higher than expected oxygen concentrations on all samples could be explained by evidence of carbonate species indicated by XRD in Table 2 and C 1*s* spectra by XPS. The presence of carbonate species is anticipated as both lithium and titania scavenge CO_2, and CO_2 was observed to desorb from postrun catalyst samples in temperature-programmed desorption (TPD) studies by us. However, the presence of carbonates does not explain the difference in the different loadings, as the higher loaded catalysts are shown in Fig. 11 and Tables 3 and 4 to have more surface carbonates. In addition, the XPS results show only titanium to be present in the 4+ oxidation state. This indicates that no $LiTiO_2$ is present on the catalyst surface of the 16.2% lithium–titania catalyst, even though the presence of this crystal structure was detected by XRD. The XPS samples were exposed to the atmosphere for an extended period of time prior to analysis, so the $LiTiO_2$ phase could have changed.

Differential Thermal Analysis

In studying the effects of temperature on the catalytic activity and product selectivity using the 16.2% lithium–titania catalyst, the post-run catalyst samples exhibited a change in their physical state. To identify a phase transition or crystal structure inversion, a differential thermal analysis (DTA) study of the 16.2% lithium–titania catalyst was performed. Samples of γ-alumina,

TABLE 4

Surface Composition of the Lithium–Titania Catalysts as Measured by X-Ray Photoelectron Spectroscopy

Catalyst	Surface composition (wt%)					Atomic ratios	
	Ti	Li	O	C	Fe	$\frac{Li}{Ti}$	$\frac{O}{Ti + Li}$
1% Li_2O/TiO_2	38.3	1.7	38.6	17.1	4.5	0.31	2.34 (1.84)
4% Li_2O/TiO_2	41.5	4.3	42.9	8.1	3.2	0.71	1.80 (1.51)
7% Li_2O/TiO_2	25.0	6.6	54.7	10.9	2.9	1.82	2.32 (1.28)
11% Li_2O/TiO_2	33.2	7.3	44.6	13.3	1.6	1.51	1.60 (1.06)
16% Li_2O/TiO_2	16.7	13.4	49.5	19.2	1.1	5.54	1.36 (0.89)

TiO_2, Li_2O, and the 16.2% lithium–titania catalyst were analyzed by DTA. The Li_2O reacted with the quartz crucible forming lithium silicate between 400 and 500°C and destroying the crucible, so the experiments with Li_2O were terminated. The γ-alumina and rutile TiO_2 showed similar results with only minor fluctuation in the differential temperature measurement attributed to noise throughout the entire temperature range (25 to 850°C). The 16.2% lithium–titania catalyst, however, exhibited an endotherm between 730 and 745°C. Figure 12 shows the differential temperature deflection observed for the 16.2% lithium–titania catalyst. This suggest that the catalyst probably undergoes a phase transition at reaction temperatures.

Infrared Analysis

The 16.2% lithium–titania catalyst was studied using DRIFT techniques. A "praying mantis" diffuse reflective attachment (Harrick Scientific) provided the optical elements required for this study. Samples were prepared by passing the material through a 50-mesh screen and filling the sample holder to a depth of about 3 mm. Figure 13 shows the spectra of the catalysts after drying (d), after pretreatment (c), and after 2 h of reaction (b). These spectra are compared to a spectrum of the catalyst that was treated in air at 800°C, spectrum (a), to induce the phase transition observed by DTA. Bulk Li carbonate has bands between 1400–1500 cm^{-1} along with a strong band at 2800–3000 cm^{-1}. Figure 13 show bands in the 1400–1500-cm^{-1} frequency, but not in the high-frequency range; thus the observed spectra might correspond to surface carbonate species. The carbonate species were also detected by XRD (Table 2), and XPS (Table 3). The spectra of the catalyst also show infrared absorption in the range where C–H, O–H, HCO_3^-, and sorbed H_2O stretches might be observed. However, since the samples were exposed to the atmosphere, the spectra cannot be related unequivocally to species present during reaction.

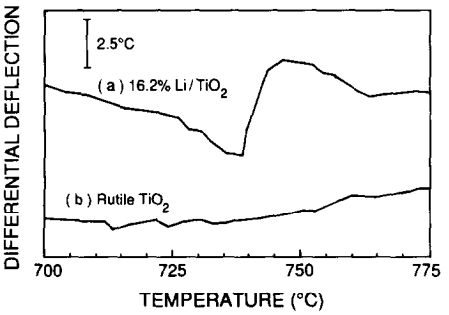

FIG. 12. Differential thermal analysis thermograms for the 16.2% lithium–titania catalyst (a) and rutile titania (b).

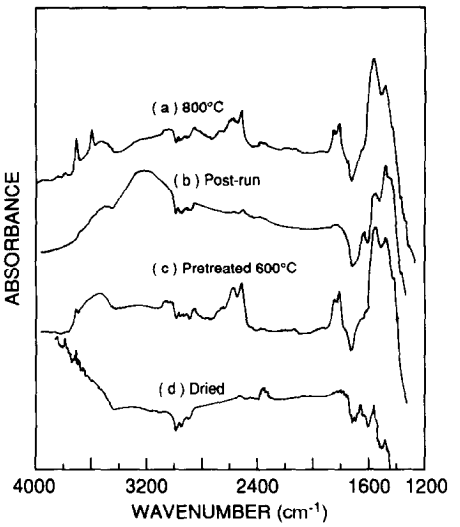

FIG. 13. Representative diffuse reflectance spectra of the 16.2% lithium–titania catalyst measured in air; (a) oven-treated at 800°C, (b) postrun catalyst sample, (c) 600°C calcination pretreatment, and (d) dried catalyst.

DISCUSSION

The results indicate that as Li_2O is added to rutile titania, hydrocarbon product yield reached a maximum for the catalyst with a 16.2% lithium loading. For these catalysts, the hydrocarbon product selectivity increased with increased lithium loading, attaining values better than results observed in the gas phase (*14*). The hydrocarbon

yield of the catalyst with a 16.2% lithium loading was significantly higher than the other catalysts studied. The nature of the surface species responsible for the high activity of this catalyst remains to be determined. The XRD results at room temperature show that $LiTiO_2$ was present only in the 16.2% lithium–titania catalyst (see Table 2). The XPS results, obtained at room temperature and shown in Table 3 and Fig. 13, indicate that there are two bands for the oxygen 1*s* transition, and their relative percentage changes with lithium loading. The ratio of O/(Li + Ti), shown in Table 4, also decreases with increasing lithium loading, suggesting that increasing lithium loading controls the amount of surface oxygen. This low-oxygen-containing surface might be relevant in attaining the high hydrocarbon yield observed using the 16.2% lithium–titania catalyst. However, these characterization results are not conclusive because the catalysts could exist in different phases at the reaction temperatures (*29, 30*). Differential thermal analysis also indicates the possible phase transition for reaction temperatures greater than 700°C for the 16.2% lithium–titania catalyst. Consequently, the characterization results obtained at present do not permit a unique determination of the active site or surface responsible for the activity results observed.

Other than the observed phase transition, the lithium–titania catalysts behave similarly to other alkali-promoted metal oxides. Thus, one can speculate that the lithium–titania catalysts have $[Li^+O^-]$ centers similar to those which have been reported by Ito *et al.* for Li/MgO catalysts. The $[Li^+O^-]$ centers were observed when the lithium replaced the Mg in the oxide crystal lattice. If it is assumed that this also holds for the lithium–titania catalyst, the increase in lithium loading must help facilitate the cation exchange giving rise to the more selective activation of methane with increased lithium loading. The 16.2% lithium–titania catalyst, which was the most active and selective catalyst, has the highest atomic ratio of Li/Ti suggesting that surface lithium concentration is important in generating $CH_3\bullet$ radicals. The transient results suggest that perhaps the 16.2% lithium–titania catalyst more readily absorbs oxygen, which then activates the selective conversion of methane. In addition, increasing the loading of lithium reduces the combustion capacity, suggesting that lithium blocks the lattice oxygen of titania which seems to lead to the nonselective products.

There seems to be a consensus that the rate-determining step is the abstraction of the first hydrogen from the methane molecule. Cant *et al.* (*31*) have shown, by isotope tracing with deuterated methane, that the rate-determining step is the breaking of the first carbon–hydrogen bond and the formation of methyl radicals. Table 5 summarizes activation energies that have been reported by several authors over various oxidative coupling catalysts and are compared to the activation energy determined for the 16.2% lithium–titania catalyst. Many reports have indicated that the catalysts have activation energies for methane conversion and for C_2^+ formation of ca. 50 kcal/mole. Since Lane and Wolf (*14*) reported an apparent activation energy in the gas phase to be 55 kcal/mole, it appears that the catalysts do little in many cases to lower the activation energy of the rate-limiting step. However, a few of the catalysts, such as the 16.2% lithium–titania catalyst, have lower activation energies than observed for gas-phase reactions. Although no methane was observed by us to be adsorbed on the lithium–titania catalyst using the dynamic flow technique, Ekstrom and Lapszewicz (*38*) have measured the adsorption of methane on the surface of Sm_2O_3. They suggest that the methane acts as a weak acid and the catalyst acts as a strong base. Thus, if any adsorbed methane exists on the lithium–titania catalyst, it should be dependent on the surface basicity and thus be a function of the degree of alkali promotion.

TABLE 5

Summary of Reported Activation Energies for the Oxidative Coupling of Methane

Reference	Catalyst	Activation energy (kcal/mole)[a]		
		CH_4 conversion	C_2^+ formation	CO_x formation
This study	Li_2O–TiO_2	—	25.6(37.6)[b]	—
Asami *et al.* (*32*)	PbO/MgO	*nr*	50.3	25.9
Ito *et al.* (*19*)	Li/MgO	55.2	*nr*	*nr*
Keulks and Yu (*33*)	Bi_2O_3–P_2O_5–K_2O	*nr*	58 (28)[c]	*nr*
Kimble and Kolts (*34*)	Li/CaO	41.8	*nr*	*nr*
Labinger and Ott (*10*)	Mn–Mg oxide	58.	*nr*	*nr*
Lane and Wolf (*14*)	Gas phase	55.	52	72.[d]
Lin *et al.* (*35*)	Na/CaO	49.0	68.8	34.5
Otsuka and Jinno (*36*)	Sm_2O_3	35.6	*nr*	*nr*
Sofranko *et al.* (*13*)	Na–Mn/MgO	49.0	47.0	*nr*

Note. *nr* indicates not reported.

[a] 1 kcal/mole = 4.184 kJ/mol.

[b] Value for low reactant partial pressure, 0.2, and value in parentheses for high reactant partial pressure, 0.8.

[c] Value for temperatures <650°C and value in parentheses valid for temperatures >650°C.

[d] Activation energy for CO formation.

To compare the 16.2% lithium–titania catalyst with other results reported in the literature, Fig. 14 was plotted to show hydrocarbon yield as a function of methane conversion. The symbol, +, depicts catalytic results reported in the literature; the straight line represents 100% hydrocarbon selectivity, and the curved line represents the gas-phase yield results reported elsewhere (*14*). The results for the 16.2% lithium–titania catalyst were superimposed and are represented by the ○ symbols. The values at high conversion were measured at low reactant partial pressures, ca. 0.15, and a short time-on-stream. Figure 14 indicates that the 16.2% lithium catalyst has the potential for competing with other catalysts reported in the literature; however, problems with deactivation must be overcome. The 16.2% lithium–titania catalyst does more than change product selectivity. Table 1 shows that it improves the space-time yield for methane conversion, and therefore enhances the rate-limiting steps. The transient results presented in Figs. 6 and 7 suggest that ethane and ethylene are produced over the catalyst by the reaction of methane and adsorbed oxygen. The catalyst also improves the product selectivity to ethylene, and Hutchings *et al.* (*37*) propose that this could possibly be due to the formation of ethylene directly from methane on the catalyst surface and not from the dehy-

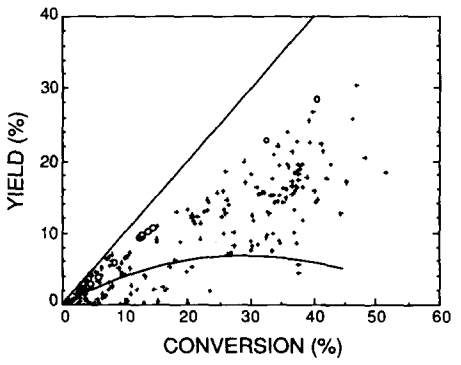

FIG. 14. Comparison of the 16.2% lithium–titania catalyst (○) with results reported in the literature (+) showing hydrocarbon yield as a function of methane conversion; straight line represents 100% hydrocarbon selectivity and curved line represents gas-phase results discussed elsewhere (*14*).

drogenation of ethane. However, the results shown in Fig. 7 suggest that only small amounts of ethylene come directly from methane.

In addition to agreeing that the breaking of the first carbon–hydrogen bond is rate limiting, most researchers suggest that the hydrocarbon-forming chemistry takes place in the gas phase. The product distribution of hydrocarbon products is similar to methane pyrolysis. Many parallels have been drawn between oxidative coupling and methane combustion and pyrolysis. The gas-phase combustion chemistry involving radical reactions is relatively well understood, and several books are available on this subject (*39–42*). Lunsford and coworkers (*43–46*), using matrix isolation electromagnetic spin resonance (MIESR) spectroscopy, have demonstrated that gas-phase methyl radicals are present in the gas phase. They have shown that surface-generated methyl radicals are important in oxidative coupling of methane, and Campbell *et al.* (*43*) reported that at least 40% of the ethane formation takes place in the gas phase. Jones *et al.* (*9*) have performed Paneth mirror experiments and confirmed that it is likely that gas-phase methyl radicals are present.

The source of the oxygenated products is even less clear. Some authors suggest that sequential combustion of ethane and ethylene is important (*9, 12, 47*) while others suggest that only ethane is combusted (*48*). In addition, carbon oxides can be generated when methyl radicals are oxidized on the catalyst surface or in the gas phase. It should be pointed out that in the presence of almost all catalysts CO_2 has been reported as the major oxidation product, whereas in the absence of a catalyst CO is the major oxidation product. The transient results suggest that CO results from methane reacting with lattice oxygen (Fig. 6) and that CO_2 and some CO results from the combustion of the ethylene (Fig. 9).

Figure 15 shows reaction pathways that are consistent with the transient and fixed-bed results and have been suggested by several authors. At present, the relative importance and role of these steps is poorly understood and may vary from catalyst to catalyst. Figure 15 depicts the generation of methyl radicals by a catalyst surface, in the gas phase by oxygen initiation, and by gas-phase radical chain propagation reactions. The transient results suggest that CH_3• radicals are generated by adsorbed oxygen over the 16.2% lithium–titania cata-

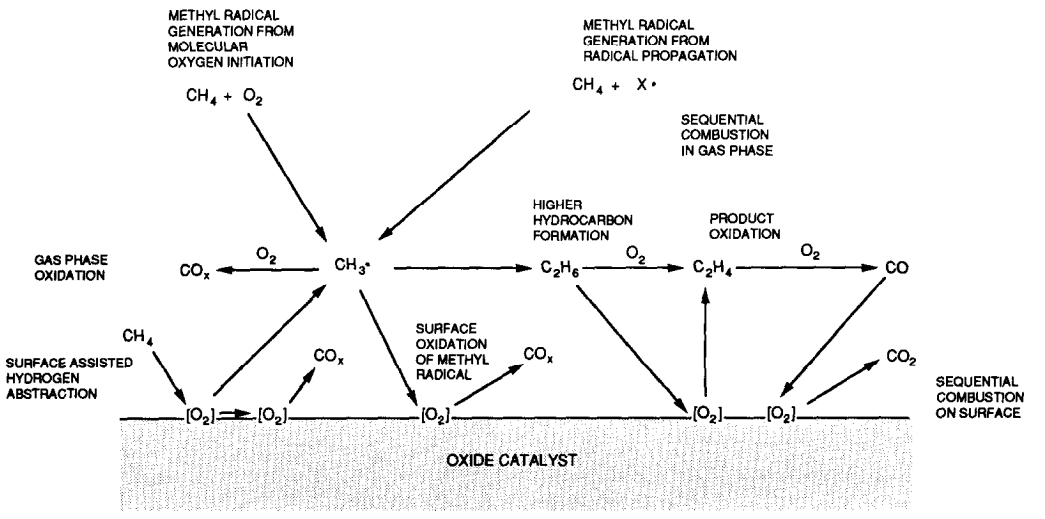

FIG. 15. Possible reaction pathways considered feasible for the oxidative coupling of methane.

lyst. In the pathway shown in Fig. 15, the hydrocarbon-forming chemistry takes place in the gas phase by recombination of methyl radicals and by degenerate branching reactions. The generation of hydrocarbons by surface reactions has not been included, because most authors suggest the gas phase controls the generation of higher hydrocarbons. Carbon monoxide and carbon dioxide are considered to be formed both in the gas phase by radical reactions with the methyl radical and by destruction of the methyl radicals on the catalyst surface reacting with lattice oxygen, as shown by the transient results in Fig. 6. In addition, as shown in Fig. 9b, ethylene leads to carbon oxides by sequential combustion, as shown on the right-hand side of Fig. 15. Many of the reactions shown in Fig. 15 are only thought to be important by several authors and clear evidence is still forthcoming. The transient results provided some insight into the importance of several of the reactions shown in Fig. 15, but the importance of these reactions might vary from catalyst to catalyst.

SUMMARY

A series of lithium-doped rutile titania catalysts was studied to determine the effect of lithium as a promoter for the oxidative coupling of methane. Of the catalysts tested, a 16.2% lithium–titania catalyst was shown to give hydrocarbon yields as high as 12.5%, but the catalyst deactivated with time-on-stream. The results of a 16.2% lithium–titania catalyst were compared with results from homogeneous reactions, and the catalyst was found to have high space-time yields. XRD, XPS, and DTA results of the catalysts suggest that increasing the degree of lithium promotion lowers the surface area, lowers the surface concentration of oxygen, and possibly creates different phases at elevated temperatures. Under several conditions, the 16.2% lithium catalyst compares favorably with other reported catalytic results and has an apparent activation energy of 25.6 kcal/mole. Transient experiments suggest that methane reacts with adsorbed oxygen to form C_2 hydrocarbons over the 16.2% lithium–titania catalyst and that the reaction of methane with lattice oxygen is nonselective. The dehydrogenation of ethane to ethylene readily occurs with either lattice, adsorbed, or gas-phase oxygen over this catalyst, and ethylene is less reactive than ethane but is converted to CO and CO_2.

ACKNOWLEDGMENTS

The authors gratefully acknowledge the Amoco Research Center, Naperville, Illinois, for providing financial support for this work. The authors also extend their thanks to Dr. T. H. Fleisch and Dr. Kaduk of the Amoco Research Center for collaborating on the XPS and XRD analyses.

REFERENCES

1. Keller, G. E., and Bhasin, M. M., *J. Catal.* **73,** 9 (1982).
2. Lane, G. S., Ph.D. dissertation, University of Notre Dame, 1988.
3. Bhasin, M. M., *in* "Studies in Surface Science and Catalysis" (D. M. Bibby *et al.*, Eds.), Vol. 36 (Methane Conversion), p. 343. Elsevier, Amsterdam, 1988.
4. Mimoun, H., *Nouv. J. Chim.* **11,** 513 (1987).
5. Roos, J. A., Bakker, A. G., Bosch, H., van Ommen, J. G., and Ross, J. R. H., *Catal. Today* **1,** 133 (1987).
6. Scurrell, M. S., *Appl. Catal.* **32,** 1 (1987).
7. Lee, J. S., and Oyama, S. T., *Catal. Rev. Sci. Eng.* **30,** 249 (1988).
8. Mars, P., and van Krevelen, D. W., *Chem. Eng. Sci. Suppl.* **3,** 41 (1954).
9. Jones, C. A., Leonard, J. J., and Sofranko, J. A., *J. Catal.* **103,** 311 (1987).
10. Labinger, J. A., and Ott, K. C., *J. Phys. Chem.* **91,** 2682 (1987).
11. Labinger, J. A., Ott, K. C., Mehta, S., Rockstad, H. K., and Zoumalan, S., *J. Chem. Soc. Chem. Commun.*, 543 (1987).
12. Sofranko, J. A., Leonard, J. J., and Jones, C. A., *J. Catal.* **103,** 302 (1987).
13. Sofranko, J. A., Leonard, J. J., Jones, C. A., Gaffney, C. A., and Withers, H. P., *Prep. Div. Pet. Chem. Amer. Chem. Soc.* **32,** 763 (1987).
14. Lane, G. S., and Wolf, E. E., *J. Catal.* **113,** 144 (1988).
15. Asami, K., Omata, K., Fujimoto, K., and Tominaga, H.-O., *J. Chem. Soc. Chem. Commun.*, 1287 (1987).

16. Hutchings, G. J., Scurrell, M. S., and Woodhouse, J. R., *J. Chem. Soc. Chem. Commun.*, 253 (1988).
17. Yates, D. J. C., and Zlotin, N. E., *J. Catal.* **111,** 317 (1988).
18. Lane, G. S., and Wolf, E. E., *J. Catal.* **105,** 386 (1987).
19. Ito, T., Wang, J.-X., Lin, C.-H., and Lunsford, J. H., *J. Amer. Chem. Soc.* **107,** 5062 (1985).
20. Hutchings, G. J., Scurrell, M. S., and Woodhouse, J. R., *J. Chem. Soc. Chem. Commun.*, 1862 (1987).
21. Kolts, J. H., and Kimble, J. B., US Patent 4,658,077 to Phillips Petroleum Co. (1987).
22. Lane, G. S., and Wolf, E. E., *in* "Proceedings, 9th International Congress on Catalysis, Calgary, 1988" (M. J. Phillips and M. Ternam; Eds.), Vol. 2, p. 949. Chem. Institute of Canada, Ottawa, 1988.
23. Larkins, F. P., and Nordin, M. R., *in* "Studies in Surface Science and Catalysis" (D. M. Bibby *et al.*, Eds.), Vol. 36 (Methane Conversion), p. 409. Elsevier, Amsterdam, 1988.
24. Otsuka, K., Liu, Q., Hatano, M., and Morikawa, A., *Chem. Lett.*, 903 (1986).
25. Korf, S. J., Roos, J. A., de Bruijin, N. A., van Ommen, J. G., and Ross, J. R. H., *J. Chem. Soc. Chem. Commun.*, 1433 (1987).
26. France, J. E., Shamsi, A., and Ahsan, M. Q., *Energy Fuels* **2,** 235 (1988).
27. Wendlandt, W. M., "Thermal Methods of Analysis. Chemical Publishing Co., New York, 1966.
28. Smothers, W. J., Chiang, Y., "Handbook of Differential Thermal Analysis." Chemical Publishing Co., New York, 1966.
29. Gicquel, C., Mayer M., and Bouaziz, R., *C. R. Acad. Sci.* **275,** 1427 (1972).
30. Roy, U., Petrov, K., Tsolovski, I., and Peshev, P., *Phys. Status Solidi A.* **44,** K25 (1977).
31. Cant, N. W., Lukey, C. A., Nelson, P. F., and Tyler, R. J., *J. Chem. Soc. Chem. Commun.*, 766 (1988).
32. Asami, K., Hashimoto, S., Shikada, T., Fujimoto, K., and Tominaga, H.-O., *Ind. Eng. Chem. Res.* **26,** 2348 (1987).
33. Keulks, G. W., and Yu, M., *React. Kinet. Catal. Lett.* **35,** 361 (1987).
34. Kimble, J. B., and Kolts, J. H., *Energy Prog.* **6,** 226 (1986).
35. Lin, C.-H., Campbell, K. D., Wang, J.-X., and Lunsford, J. H., *J. Phys. Chem.* **90,** 534 (1986).
36. Otsuka, K., and Jinno, K., *Inorg. Chim. Acta.* **121,** 237 (1986).
37. Hutchings, G. J., Woodhouse, J. R., and Scurrell, M. S., *in* "Proceedings, 9th International Congress on Catalysis, Calgary, 1988" (M. J. Phillips and M. Ternam, Eds.), Vol. 2, p. 923. Chem. Institute of Canada, Ottawa, 1988.
38. Ekstrom, A., and Lapszewicz, J. A., *J. Chem. Soc. Chem. Commun.*, 797 (1988).
39. Gardiner, W. C., Ed., "Combustion Chemistry." Springer–Verlag, New York, 1984.
40. Glassman, I., "Combustion." Academic Press, New York, 1977.
41. Hucknall, D. J., "Chemistry of Hydrocarbon Combustion," Chapman & Hall, London, 1985.
42. Lifshitz, A., Ed., "Shock Waves in Chemistry." Dekker, New York, 1981.
43. Campbell, K. D., Morales, E., and Lunsford, J. H., *J. Amer. Chem. Soc.* **109,** 7900 (1987).
44. Driscoll, D. J., Martir, W., Wang, J.-X., and Lunsford, J. H., *J. Amer. Chem. Soc.* **107,** 58 (1985).
45. Driscoll, D. J., and Lunsford, J. H., *J. Phys. Chem.* **89,** 4415 (1985).
46. Driscoll, D. J., Campbell, K. D., and Lunsford, J. H., *in* "Advances in Catalysis (D. D. Eley, P. W. Selwood, and Paul B. Weisz, Eds.), Vol. 35, p. 139. Academic Press, New York, 1987.
47. Ali Emesh, I. T., and Amenomiya, Y., *J. Phys. Chem.* **90,** 4785 (1986).
48. Otsuka, K., *Sekiyu Gakkaishi* **30,** 385 (1987).